Deep Learning Models for Flood Detection in Nepal: Challenges and Insights

Amit Bhattarai[1,2] ✉, Ranju Kumari Shiwakoti[2]

[1]Tribhuvan University, Mahendra Ratna Campus, Tahachal, Kathmandu.

amit.bhattarai@mrc.tu.edu.np

[2]Tribhuvan University, Pulchowk Campus, Pulchowk, Lalitpur

Received: July 8, 2025 Accepted: June 6, 2026 Published: July 15, 2026

DOI: https://doi.org/10.3126/thj.v18i1.97713

Abstract

Climate-driven increases in flood frequency and intensity have made rapid and reliable flood monitoring essential for effective emergency response. Synthetic Aperture Radar (SAR) imagery from Sentinel-1 is particularly valuable for this purpose because it operates independently of cloud cover and illumination conditions, enabling flood observation during extreme weather events. In this study, a 5-channel U-Net was developed for flood mapping in Nepal, using multi-temporal Sentinel-1 SAR data and hydrologically relevant topographic information. The input configuration combined pre-flood VV and VH backscatter, post-flood VV and VH backscatter, and Height Above the Nearest Drainage (HAND) data to improve the discrimination of flooded and non-flooded areas. The model demonstrated stable convergence during training, with continuously decreasing loss and improving Dice and IoU scores on both training and validation datasets. Quantitative evaluation showed that the proposed model achieved an Intersection over Union (IoU) of approximately 0.51, an F1-score of 0.67, precision of 0.68, recall of 0.66, near-perfect specificity, and an AUC of 0.996, indicating excellent class separability and strong suppression of false positives. Qualitative assessment further confirmed that the predicted inundation patterns were spatially coherent and closely matched the reference flood masks, although some local boundary overestimation and omission of small fragmented flood patches remained. These results demonstrate that integrating multi-temporal SAR backscatter with HAND in a U-Net framework provides a robust and operationally relevant approach for flood extent mapping in cloud-prone regions.

Keywords*:* Class imbalance, deep learning, disaster management, flood mapping, semantic segmentation, Sentinel-1, U-Net

Introduction

Climate change causes the ferocity of extreme weather, the entire field of global disaster management is shifting gears, with floods, landslides and melting of snow standing out as the most glaring examples. Devastation is jaw-dropping: from 2008 to 2017, floods alone made up 41 percentage of all natural disasters (Kumar et al., 2025), and they've driven the lion's share of over 1 trillion US Dollar in worldwide damages since 1980 (Tao et al., 2024). To the mountains, developing countries are hardest hit by the situation. In Nepal rare mixture of steep landforms, very heavy monsoon rains, and the earth's movements create one of the most dangerous places on earth. This leads to annual economic losses of about NRS 9 Arab (Yadav, 2024), a fact that emphasizes the immediate need for stronger prevention measures. Present disaster management systems are limited and rely on manual field surveys and post-event assessments which causes delay which falls during critical response time (Gandhi et al., 2024).

This research relies on technological foundations while addressing three persistent gaps in the literature: (1) insufficient validation of hybrid physics-ML models in developing world contexts; (2) operational challenges in last-mile warning dissemination; and (3) policy-implementation disconnects in centralized governance systems. It specifically focuses on developing and evaluating a deep learning model for flood detection using Sentinel-1 SAR imagery, aiming to improve the speed, accuracy, and scalability of flood monitoring in different part of Nepal for quick response.

Theoretical Framework

Floods are one of the most common and most destructive natural disasters that occur all over the world and every year they cause huge economic losses, infrastructure destruction, and human deaths (Smith, 2020; Wang & Zhang, 2021). Climate change and rapid urbanization are the main factors responsible for the increasing frequency and intensity of these disasters and the need for effective flood monitoring systems that are able to respond quickly has become more pressing (Johnson et al., 2019; UNDRR, 2022). Remote sensing, particularly the use of satellite imagery, has become a powerful method for flood detection over large areas, however, traditional techniques still have problems when it comes to speed, accuracy, and flexibility of use (Brown et al., 2021; Chen & Liu, 2022).

Multi-source data SAR, optical imagery, DEMs, and social media images are refined to sharpen contextual insights and improve overall precision (Kumar & Singh, 2022; Zhou, 2023).

Since the data are stubbornly diverse and mismatched Co-ordinate Reference System (CRS), it causes challenges in real time fusion (Lee et al., 2022). These issues are better conceptualization which leads to effectiveness of flood monitoring systems to maximum (Robinson, 2022). Even though deep learning model with multi-source data fusion has significant potential for identifying the flood area and addressing reliability concern of automation, and variability challenges which can be solved by monitoring and detection (Thompson, 2023; UNDRR, 2023).

Related Works

The increasing effect of climate change, particularly through hydrological and mass-wasting hazards. It is greatly altering the global disaster management frameworks. An empirical study by Kumar et al. (2025) shows a disconcerting trend. Natural disasters between 2008 and 2017, flood accounts for 41 percentage. More than one trillion dollars damage was done since 1980 (Tao et al., 2024).

Nepal also faces huge economic losses which accounts for more than NRS 9 Arab (Yadav, 2024) yearly, which indicates more effective mitigation strategies should be implemented to minimize human and economic loss. Bayesian neural networks and hybrid techniques helps to increase confidence score on forecasts (Lakshminarayanan et al., 2017; Schwegmann et al., 2020).

This study develops a detailed plan for identifying floods, utilizing deep learning to map out the water and detect it instead of manual method. It hinges on four tied-together pieces that create an integrated workflow for analyzing and disaggregating.

Data Acquisition and Preprocessing Module

This initial phase aims to collect and prepare data as it is yet again important tests of product data performance. For example, the mobile Earth Watch system has been in operation for over a decade now with focus on First. A system is even now responsible for capturing Sentinel-1 SAR (Synthetic Aperture Radar) imagery automatically. One of the advantages of SAR is that it can penetrate clouds. Therefore, when traditional optical satellites are often obscured during the monsoon season, SAR will still be effective for monitoring. This has been a flood mapping technique long established in remote sensing (Twele et al., 2016; Yang et al., 2021).
Following acquisition, geometric and radiometric preprocessing are applied to SAR data to ensure accuracy, consistency and then stored for data handling.

Deep Learning Processing Core

The advanced deep learning model in the middle of the framework serves as a flood detector. For its ability to classify at the pixel level, we choose the U-Net structure as the base model (Ronneberger et al., 2015), a very effective deep learning architecture that has been first introduced for medical image segmentation. This architecture has also been proved for effectiveness in a flood extent extraction from satellite images (Konapala & Kumar, 2021; Mesvari & Shah-Hosseini, 2023). A Focal Loss and Dice Loss based composite loss function is used to handle the heavy class imbalance pairs (there are much fewer flooded than there's non flooded in images) that coexist with flood images (Biswas, 2022). This strategy allows the model to accurately locate smaller critical flood regions based on cross-entropy and Dice-based loss concept (Lin et al., 2017; Yeung et al., 2022). Accordingly, the SAR image is automatically processed by a deep learning model and unnecessary parts of an image are discarded to display floodwaters.

Validation and Accuracy Assessment

To ensure the reliability of the flood maps, a multi-faceted validation process is implemented and flood maps generated from SAR data are validated against Sentinel-2 optical imagery, providing an independent verification of the results. Furthermore, ground truth data is used to further verify the accuracy of the detected flood extents. Different metrics, including Intersection over Union (IoU), Precision, and Recall provide a comprehensive measurement of model accuracy.

Operational Output and Dissemination

Providing correct information to stakeholders in a timely manner allows for action. The most recent and ever evolving situation can be tracked to map of the extent of flooding. The system's ability to automatically generate alert for the disaster management department is its more crucial. This frame ability to detect floods is also significant improvement over conventional techniques. It is a great achievement in the field of flood monitoring and detection, especially for mountainous region like Nepal where AI with Sentinel-1 SAR data is used to monitor the flood (UNOOSA, 2021). The fact that the system can operate well even during strong cloud cover and treat unbalanced datasets. It will also be an indispensable tool for development of early flood warning systems, and thus a means to mitigate the devastating effects of floods (Van Esch et al., 2021).

Data Processing and Analytics Core

Raw data undergo comprehensive pre-processing, harmonization, and integration to implements advanced deep learning models for predictive analysis.

Research Methodology

The methodology uses multi-modal data acquisition, a comprehensive preprocessing pipeline, neural network architecture. This study is rigorous, multi-stage methodology designed for the development and evaluation of a deep learning for floodwater segmentation. The methodology uses multi-modal data acquisition, a comprehensive preprocessing pipeline, neural network architecture.

Data Acquisition and Ground Truth Generation

The foundation of this research is a multi-modal dataset integrating satellite-based radar imagery with topographic data to detect and analysis of flood.

Figure 1. *Flood Detection Workflow*

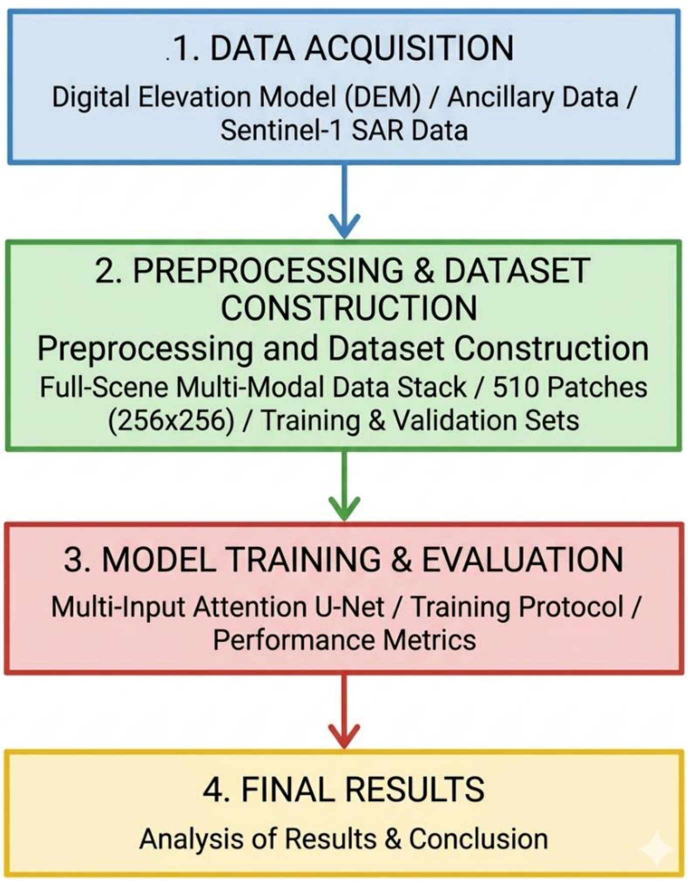

Primary Data Source (Sentinel-1).

Sentinel-1's C-band Synthetic Aperture Radar (SAR), which is mission-critical for flood monitoring was primary data source. Its ability to pierce cloud over is constant throughout year. Dual polarization backscatter (VV and VH) coefficients were used in the Ground Range Detected (GRD) data. These polarizations server as foundation for flood detection because they are extremely sensitive to the from water on the ground.

Ancillary Data Source (Digital Elevation Model).

Essential topographic features were provided by integrating Digital Elevation Model (DEM). Elevation, slope, aspect, Topographic wetness index (TWI) and Hand Above Nearest Drainage (HAND)were all extracted from DEM. It helps to distinguish flood water from SAR artifacts such as in complex terrain and shadow by enabling the model to learn geomorphological vulnerabilities to flooding.

Ground Truth Generation.

The reference data for model training and validation consisted of a meticulously generated binary flood mask which was created through the manual annotation of the flood event, primarily using concurrent high-resolution optical imagery from Sentinel-2 during periods of before flood event where visibility is high and cloud particle are less than 10 percentage where visual is clear. To further enhance accuracy and resolve ambiguities, the initial masks were validated and refined using verified by using ground observations.

Data Preprocessing and Dataset Construction

The raw data was preprocessing and partition to prepare it for deep learning. Major flood event on 2 October 2024 in the Nawalpur district of Nepal was use to analysis, train and validation of model.

Dataset Characteristics

The initial, full-scene dataset was characterized by its large dimensions and significant class imbalance due to high no of non-flood pixel present on it. The input Sentinel-1 SAR image had dimensions of (3910, 8851, 3), comprising the VV, VH, and a derived ratio channel whereas topographic feature stack had dimensions of (3910, 8851, 5).

Patch Extraction and Partitioning. To ensure computational feasibility and effective learning, the full-image data was partitioned into smaller 256x256 pixel patches and total of 510 image-and-feature patches with their corresponding masks were extracted. Training and validation sets contained representative flood examples, resulting in 80-20 split for training and validation:

Dataset Partitioning. 407 patches contain 148 flood positive samples, whereas in validation 103 patches contain 38 flood-positive samples

Model Architecture: Multi-Input Attention U-Net

Multi-Input Attention U-Net architecture was implemented for parallel data stream processing and feature recalibration.

Figure 2. *U-Net architecture*

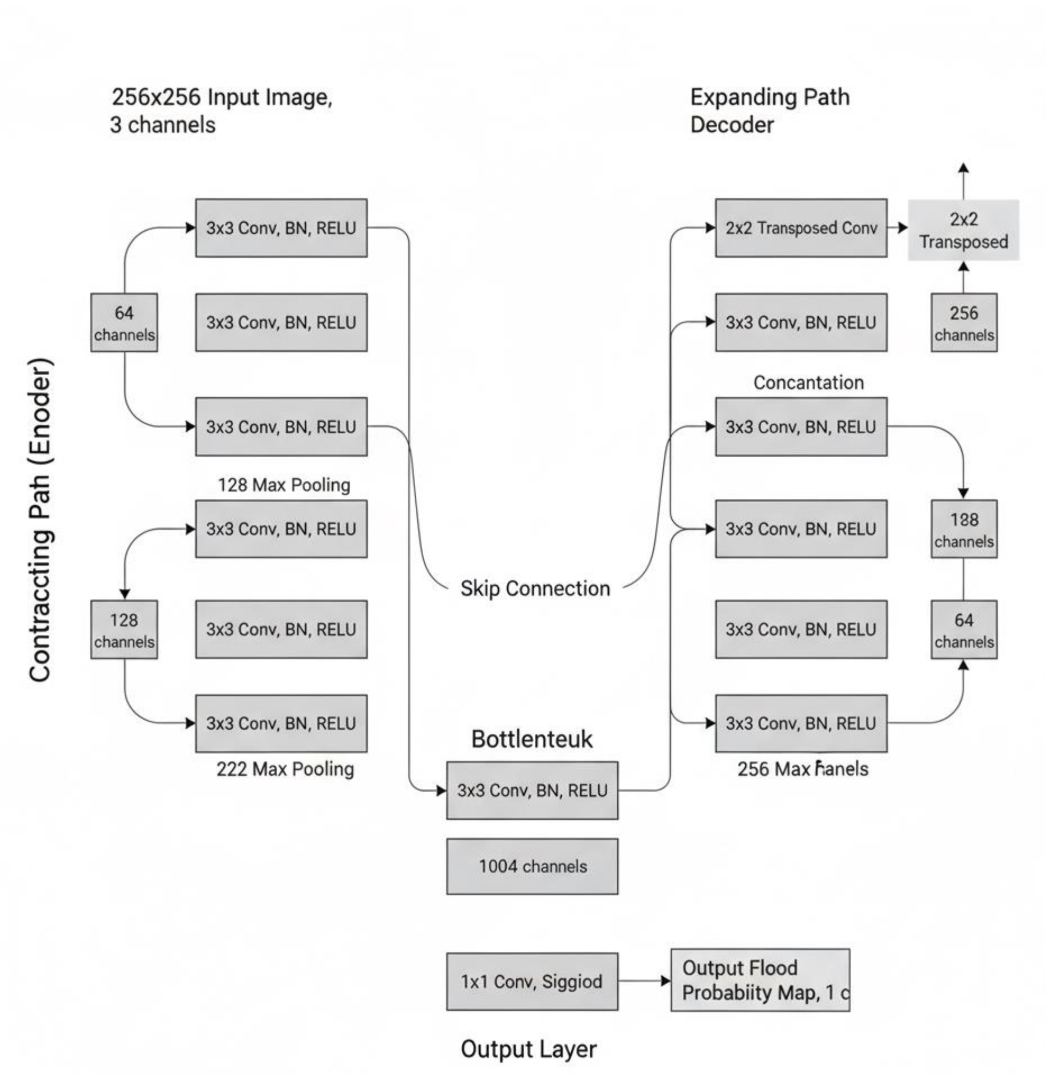

U-Net Foundation. The architecture is based on the encoder-decoder structure of U-Net, featuring skip connections that pass high-resolution spatial information from the encoder to the decoder for accurate pixel-level boundary segmentation.

Multi-Input Branches. Two input branches run in parallel along the beginning of encoder stage. One branch handles the 3-channel Sentinel-1 SAR data and another handles the 5-channel topographic feature stack. These streams are passed through separate convolutional layers before fusion, in order for the model to learn modality-specific representations.

Attention Gates. Attention gates are integrated into the skip connections. These gates learn to re-weight the feature maps being passed from the encoder to the decoder, adaptively focusing on the most salient features for flood detection while suppressing irrelevant background noise or artifacts.

Model Capacity. The final architecture is a deep network providing significant capacity of approximately 31.8 million trainable parameters to learn the complex relationships between SAR backscatter, topography, and flood presence.

Training and Evaluation Protocol

The model was trained for 50 epochs on a system equipped with a single GPU in a google colab which was designed for stability and convergence on the highly imbalanced dataset.

Loss Function. Focal Loss and Dice Loss was employed to address extreme class imbalance by down-weighting the loss attributed to well-classified majority-class pixels (Focal Loss) while directly optimizing for segmentation overlap (Dice Loss).

Optimizer and Learning Rate. Initial learning rate of 1.0e-5 was used which is called Adam optimizer.

Model Check point. The model's weights were saved only when the validation Intersection over Union (val_iou_metric) improved, to ensuring that the final model represents the best-performing state.

Reduce LROnPlateau. The learning rate was dynamically reduced if the validation metric stagnated, allowing for finer-grained optimization as the model approached convergence.

Early Stopping. A patience-based early stopping mechanism prevents unnecessary training and potential overfitting while training.

Evaluation Metrics. Model performance was comprehensively assessed using, Intersection over Union (IoU), Precision, Recall, and F1-Score. Among different evaluation metrices IoU metric on the validation set was the primary indicator that was used for model selection and final performance reporting.

Results

The improved "Multi-Input-Attention-UNet" model was trained for 50 epochs on the processed dataset of Sentinel-1 images and topographic layers from DEM. The performance of the model was measured on both training and validation datasets using Intersection over Union (IoU), Precision, Recall, F1-Score and Loss.

The results of the training process presented a steady but rather limited increase through the 50 epochs. The best performance of our model is at after the final epoch (i.e., Epoch 50), where the value of validation IoU metric reaches to its maximum. After final epoch, the last set of validation set key metrics were:

Quantitative Validation Metrics U-Net

Validation IoU. Approximately 0.507

Validation Precision. Approximately 0.683

Validation Recall. Approximately 0.663

Validation F1-Score. Approximately 0.672

Analysis of Model Behavior and Challenges

Evaluation of the epoch-by-epoch training provides several key insights into the model's learning behavior and final performance.

Figure 3. *IoU Metric*

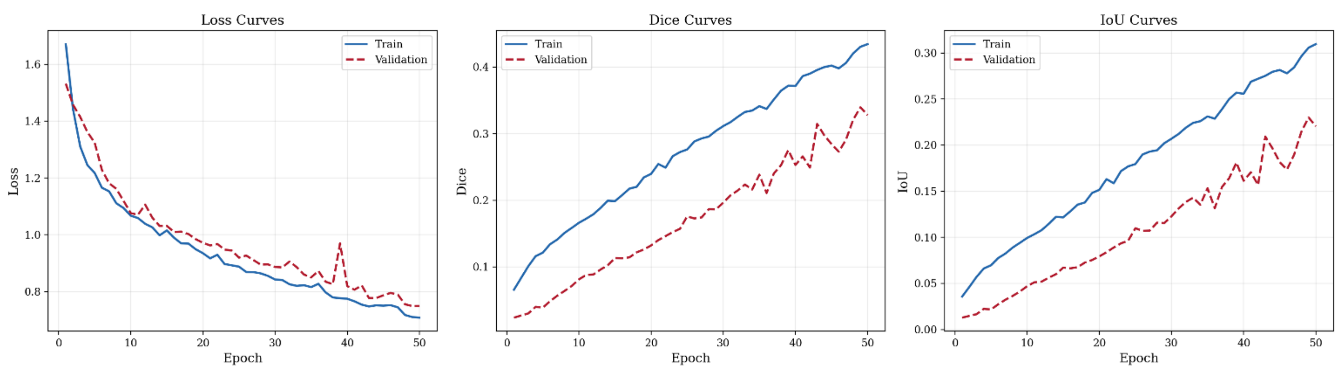

Figure 3 illustrates the dynamics of training and validation learning of the proposed U-Net model over 50 epochs in terms of loss, Dice coefficient, and Intersection over Union (IoU). The trend in loss curves is consistently decreasing in both training and validation, which means that the optimization is stable, and the segmentation error decreases gradually during training. Meanwhile, the Dice and IoU curves grow steadily in both sets, which validates the fact that the model becomes more and more effective in outlining the region of flooding. Despite the fact that the training curves are still higher than the validation curves of Dice and IoU, and the loss curve is lower, the difference between the two ones remains moderate, which implies acceptable generalization as opposed to drastic overfitting. The small variations in the validation curves during later epochs are anticipated to arise in flood mapping tasks because of the spatial heterogeneity and imbalance in class representation of validation patches. In general, the figure illustrates that the U-Net is converging and attains increasingly better segmentation accuracy on unseen data.

Figure 4. *Quantitative Performance of U-Net*

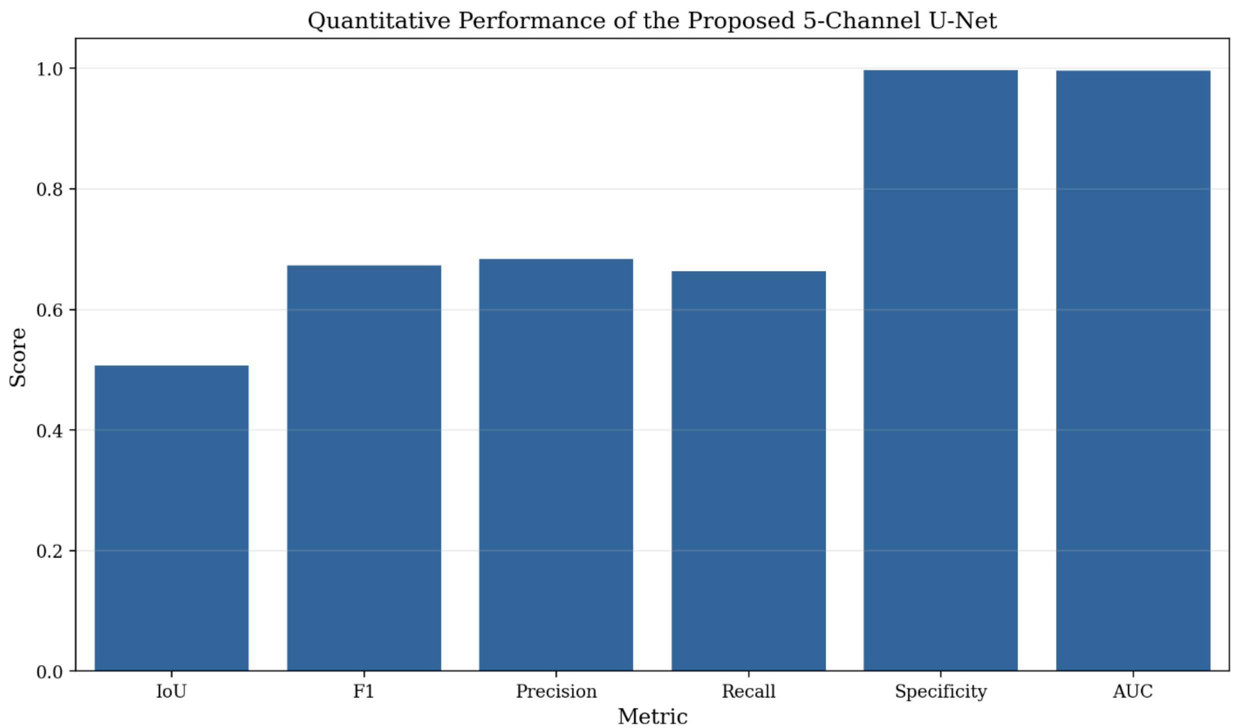

Figure 4 presents the results of the quantitative performance of the proposed 5-channel U-Net in terms of six evaluation metrics. The model obtained an IoU of about 0.51 and an F1-score of about 0.67, which implies that there is a good overlap of the predicted and reference flood extents, but IoU is more conservative as it is stricter in punishing false positives and false negatives. Precision and recall are also in good balance, with values of about 0.68 and 0.66, respectively, which indicates that the model is capable of identifying instances of flooded areas with a fair trade-off between commission and omission errors. Most significantly, specificity reaches almost 1.0, which shows that the model is very useful in the accurate detection of non-flooded pixels and minimizing false alarms, whereas the AUC of approximately 0.996 shows a perfect overall separability between flooded and non-flooded classes.

Figure 5. *Roc curve of U-Net*

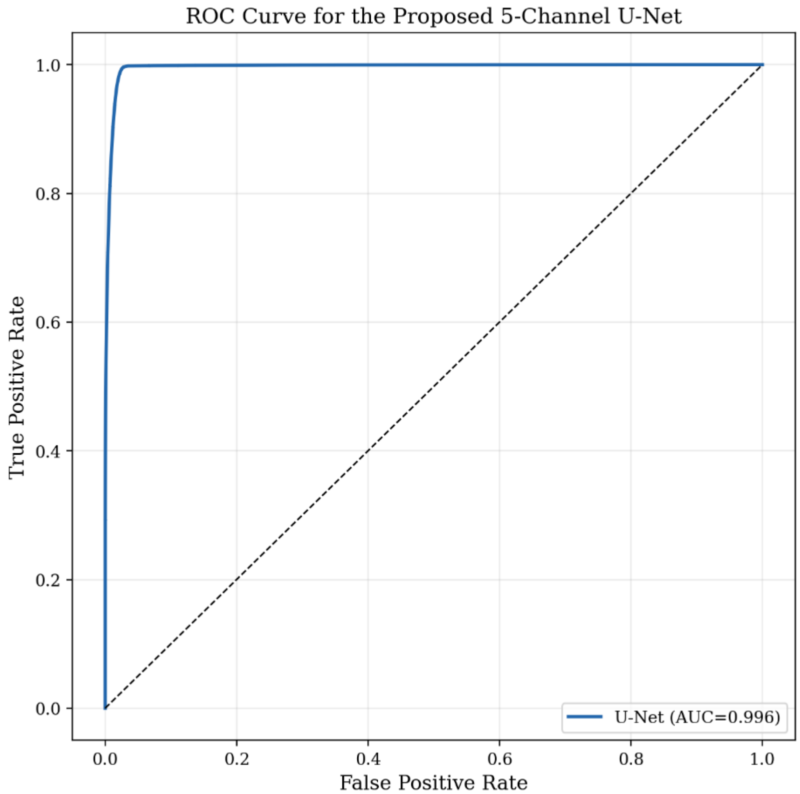

Figure 5 shows the ROC curve of the proposed 5-channel U-Net and additional proves the high discriminative performance of the model. The curve steeply increases to the upper-left corner and is much higher than the diagonal reference line that indicates random classification, which means that the model has a very high true positive rate with a very low false positive rate over the threshold settings. The AUC value of 0.996 indicates that the model ranks almost perfectly, i.e. the model is very much capable of differentiating between flood and non-flood pixels regardless of the operating threshold that one chooses. A combination of the ROC behavior and near-unity AUC demonstrates that the proposed U-Net offers robust and reliable probabilistic flood mapping performance that can be used to produce high-quality scientific reporting.

Figure 6. *After flood SAR, Ground Truth, U-Net Prediction*

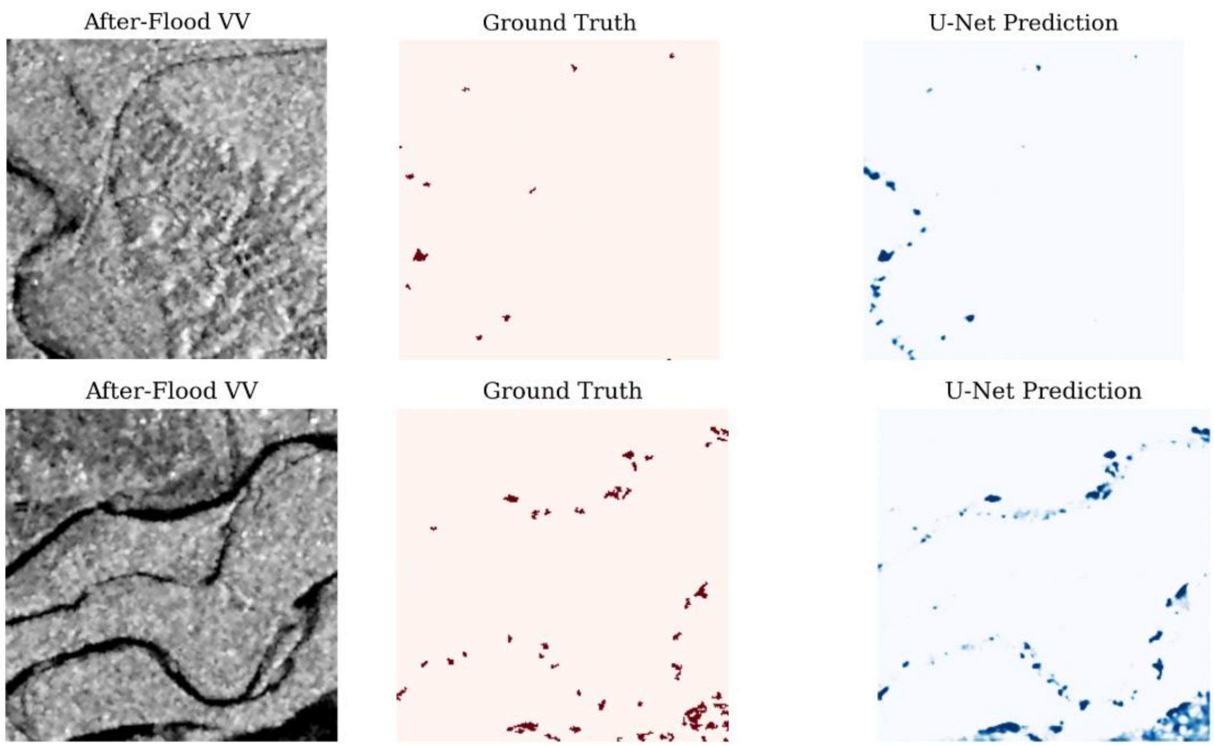

These qualitative results compare the after-flood VV SAR backscatter, the reference flood mask, and the resulting U-Net prediction and show that the model effectively captures the overall spatial distribution and shape of flood affected regions and maintains the key structures of the floods in view in the ground truth. The forecasted flood areas in both samples are widely consistent with the reference patches, especially in the long and broken flooding areas, which suggests that the model can learn significant flood patterns utilizing the SAR input. Meanwhile, certain discrepancies can be observed between prediction and reference, such as slight overestimation in some of the boundary regions, and the absence of some smaller isolated flood pixels, which is anticipated in patch-based semantic segmentation of heterogeneous landscapes. All in all, the two images show that the proposed U-Net can generate spatially consistent and visually realistic flood maps, and the ground truth is largely consistent with the local-scale mistakes.

Discussion

The findings show that the proposed 5-channel U-Net has converged and good flood/non-flood discrimination, which is reflected by the loss gradually reducing, the Dice and IoU gradually increasing, and the extremely high AUC of 0.996. This result is aligned with recent SAR-based flood-mapping studies, in which deep learning models, particularly U-Net-style networks, have been demonstrated to perform well at extracting inundation patterns on Sentinel-1 images even in challenging conditions (Nemni et al., 2020; Katiyar et al., 2021; Pech-May et al., 2023). The acquired IoU (approximately 0.51) and F1-score (approximately 0.67) indicate a sufficient balance between overlap accuracy and class separation, but it should be directly compared with prior research with caution due to a significant difference between flood datasets in terms of geography, quality of labels, class imbalance, patch design, and validation strategy (Amitrano et al., 2024). The ROC curve also confirms that the model is quite effective in the separation of flooded and non-flooded pixels over thresholds, and the specificity of the model is close to unity, which is particularly relevant in SAR flood mapping where smooth non-flood surfaces can be falsely detected as water (Tiampo et al., 2022).

The use of HAND as an additional topographic input along with pre- and post-flood VV/VH backscatter is of particular importance in this study. This has hydrological significance in that HAND is the relative vertical location to the closest drainage network, and thus it has a direct relationship with the terrain in terms of flood prone area and lateral water movement (Nobre et al., 2011). Other past researchers have also indicated that the ancillary variables like elevation, slope, and HAND may enhance flood delineation with or without SAR intensity information, particularly to reduce spurious detections and diminish physically plausible inundation patterns (Katiyar et al., 2021; Tiampo et al., 2022). The qualitative results of your figures can be interpreted in this way: the model includes the key flooded structures and maintains the overall geometry of these structures, yet still demonstrates slight overestimation at certain boundaries and lack of small fragmented areas. The same kind of behavior is also frequently observed in SAR-based segmentation literature where imbalanced classes, speckle, and fractured flood shapes complicate the recovery of the exact boundaries despite a high detection performance in general (Abbasi et al., 2023; Amitrano et al., 2024). In general, the suggested 5-channel U-Net can thus be regarded as an effective and scientifically justifiable method of flood-mapping, and the primary asset of the proposed method is the quality of the discrimination and the ability to predict the delimitation of the flooded areas in a consistent way, whereas potential future enhancements include the ability to draw the boundaries more precisely and the ability to recover small, isolated objects of floods.

Conclusion

To sum up, the proposed 5-channel U-Net has shown that a combination of multi-temporal Sentinel-1 SAR backscatter (before VV, before VH, after VV, after VH) and HAND-derived topographic information can establish a solid and efficient framework when mapping a flood extent. The model demonstrated a stable convergence during the training process, a high level of discriminatory performance, as indicated by near-perfect AUC, and a balanced ability to segment in terms of the IoU, F1-score, precision, and recall, with the qualitative results indicating that the inundation patterns predicted were spatially coherent and largely aligned to the reference flood masks. These results suggest that adding SAR intensity data with hydrologically significant ancillary terrain variables has the potential to significantly enhance the reliability and interpretability of flood mapping models, especially by aiding in more effectively damping false alarms in non-floods. In practical terms, the suggested solution has high chances of functioning as a disaster monitoring tool and instant flood assessment, particularly in areas that are prone to clouds where the SAR imagery is one of the most reliable tools of remote sensing.

References

Abbasi, M., Shah-Hosseini, R., & Aghdami-Nia, M. (2023). Sentinel-1 polarization comparison for flood segmentation using deep learning. *Proceedings, 87*(1), 14. https://doi.org/10.3390/IECG2022-14069

Amitrano, D., Di Martino, G., Di Simone, A., & Imperatore, P. (2024). Flood detection with SAR: A review of techniques and datasets. *Remote Sensing, 16*(4), 656. https://doi.org/10.3390/rs16040656

Biswas, M. (2022, July 31). Multiclass segmentation for different loss functions (Dice loss, Focal loss, total loss = summation of Dice and Focal loss) in TensorFlow. *Medium.* https://medium.com/@mb16biswas/multiclass-segmentation-for-different-loss-functions-dice-loss-focal-loss-total-loss-summation-455178517cea

Bonafilia, D., Tellman, B., Anderson, T., & Issenberg, E. (2020). Sen1Floods11: A georeferenced dataset to train and test deep learning flood algorithms for Sentinel-1. In *Proceedings of the IEEE/CVF Conference on Computer Vision and Pattern Recognition Workshops (CVPRW 2020)* (pp. 835–845). https://doi.org/10.1109/CVPRW50498.2020.00113

Boschetti, M., Nutini, F., Brivio, P. A., Bartholomé, E., Stroppiana, D., & Hoscilo, A. (2013). Identification of environmental anomaly hot spots in West Africa from time-series of NDVI and rainfall. *ISPRS Journal of Photogrammetry and Remote Sensing, 78*, 26–40. https://doi.org/10.1016/j.isprsjprs.2013.01.003

Bovolo, F., & Bruzzone, L. (2007). A split-based approach to unsupervised change detection in large-size multitemporal images: Application to tsunami-damage assessment. *IEEE Transactions on Geoscience and Remote Sensing, 45*(6), 1658–1670. https://doi.org/10.1109/TGRS.2007.895835

Centre for Research on the Epidemiology of Disasters & United Nations Office for Disaster Risk Reduction. (2020). *The human cost of disasters: An overview of the last 20 years (2000–2019).* https://www.undrr.org/publication/human-cost-disasters-overview-last-20-years-2000-2019

Chini, M., Hostache, R., Giustarini, L., & Matgen, P. (2017). A hierarchical split-based approach for parametric thresholding of SAR images: Flood inundation as a test case. *IEEE Transactions on Geoscience and Remote Sensing, 55*(12), 6975–6988. https://doi.org/10.1109/TGRS.2017.2737664

Katiyar, V., Tamkuan, N., & Nagai, M. (2021). Near-real-time flood mapping using off-the-shelf models with SAR imagery and deep learning. *Remote Sensing, 13*(12), Article 2334. https://doi.org/10.3390/rs13122334

Konapala, G., Kumar, S. V., & Ahmad, S. K. (2021). Exploring Sentinel-1 and Sentinel-2 diversity for flood inundation mapping using deep learning. *ISPRS Journal of Photogrammetry and Remote Sensing, 180*, 163–173. https://doi.org/10.1016/j.isprsjprs.2021.08.016

Lakshminarayanan, B., Pritzel, A., & Blundell, C. (2017). Simple and scalable predictive uncertainty estimation using deep ensembles. *Advances in Neural Information Processing Systems, 30*, 6405–6416. https://proceedings.neurips.cc/paper/2017/hash/9ef2ed4b7fd2c810847ffa5fa85bce38-Abstract.html

Lin, T.-Y., Goyal, P., Girshick, R., He, K., & Dollár, P. (2017). Focal loss for dense object detection. In *Proceedings of the IEEE International Conference on Computer Vision (ICCV 2017)* (pp. 2999–3007). IEEE. https://doi.org/10.1109/ICCV.2017.324

Mesvari, M., & Shah-Hosseini, R. (2023). Flood detection based on UNet++ segmentation method using Sentinel-1 satellite imagery. *Earth Observation and Geomatics Engineering, 7*(1). https://doi.org/10.22059/eoge.2023.359463.1139

Nemni, E., Bullock, J., Belabbes, S., & Bromley, L. (2020). Fully convolutional neural network for rapid flood segmentation in synthetic aperture radar imagery. *Remote Sensing, 12*(16), Article 2532. https://doi.org/10.3390/rs12162532

Nobre, A. D., Cuartas, L. A., Hodnett, M., Rennó, C. D., Rodrigues, G., Silveira, A., Waterloo, M., & Saleska, S. (2011). Height above the nearest drainage: A hydrologically relevant new terrain model. *Journal of Hydrology, 404*(1–2), 13–29. https://doi.org/10.1016/j.jhydrol.2011.03.051

Otsu, N. (1979). A threshold selection method from gray-level histograms. *IEEE Transactions on Systems, Man, and Cybernetics, 9*(1), 62–66. https://doi.org/10.1109/TSMC.1979.4310076

Pech-May, F., Aquino-Santos, R., & Delgadillo-Partida, J. (2023). Sentinel-1 SAR images and deep learning for water body mapping. *Remote Sensing, 15*(12), Article 3009. https://doi.org/10.3390/rs15123009

Ronneberger, O., Fischer, P., & Brox, T. (2015). U-net: Convolutional networks for biomedical image segmentation. In N. Navab, J. Hornegger, W. M. Wells, & A. F. Frangi (Eds.), *Medical Image Computing and Computer-Assisted Intervention – MICCAI 2015* (pp. 234–241). Springer. https://doi.org/10.1007/978-3-319-24574-4_28

Tiampo, K. F., Huang, L., Simmons, C., Woods, C., & Glasscoe, M. T. (2022). Detection of flood extent using Sentinel-1A/B synthetic aperture radar: An application for Hurricane Harvey, Houston, TX. *Remote Sensing, 14*(9), Article 2261. https://doi.org/10.3390/rs14092261

Twele, A., Cao, W., Plank, S., & Martinis, S. (2016). Sentinel-1-based flood mapping: A fully automated processing chain. *International Journal of Remote Sensing, 37*(13), 2990–3004. https://doi.org/10.1080/01431161.2016.1192304

United Nations Nepal Information Platform. (n.d.). *UNOSAT S-1 flood AI monitoring dashboard (Nepal).* Retrieved April 12, 2026, from https://un.org.np/unosat-s-1-flood-ai-monitoring-dashboard-nepal

United Nations Office for Disaster Risk Reduction. (2022). *Our world at risk: Transforming governance for a resilient future* (Global Assessment Report on Disaster Risk Reduction 2022). https://www.undrr.org/gar/gar2022-our-world-risk-gar

van Esch, S., van den Homberg, M., & Boersma, K. (2021). Looking beyond the data: An assessment of the emerging data ecosystem of Nepal's flood early warning systems. In A. Adrot, R. Grace, K. Moore, & C. W. Zobel (Eds.), *ISCRAM 2021 Conference Proceedings: 18th International Conference on Information Systems for Crisis Response and Management* (pp. 282–293). Virginia Tech. http://idl.iscram.org/files/stellavanesch/2021/2333_StellavanEsch_etal2021.pdf

Yeung, M., Sala, E., Schönlieb, C.-B., & Rundo, L. (2022). Unified focal loss: Generalising Dice and cross entropy-based losses to handle class imbalanced medical image segmentation. *Computer Methods and Programs in Biomedicine, 218*, Article 106727. https://doi.org/10.1016/j.cmpb.2022.106727